

Finite element modelling of ion convection by electrostatic forces

G. Deliège, F. Henrotte, W. Deprez and K. Hameyer

Abstract: Different formulations for the problem of a cloud of ions convected by electrostatic forces are presented. Their influence on the ionic charge conservation is discussed. It is shown that a mixed electrostatic formulation is the most accurate for the studied example.

1 Introduction

The numerical analysis of an electrostatic painting process [1] requires the solution of the classic electrostatic equations coupled with a charge conservation equation:

$$\partial_t \rho_i + \nabla \cdot \mathbf{j} = 0 \quad (1)$$

where ρ_i is the ion charge density. The purpose of this work is to determine whether the current density is preferably expressed as $\mathbf{j} = \mu \varepsilon^{-1} \mathbf{d} \rho_i$ or $\mathbf{j} = \mu \rho_i \mathbf{e}$. At the discrete level, the first expression ensures continuity of the normal component of \mathbf{j} , across material discontinuities and inter-element boundaries, which is the natural continuity for a flux density (here a flux of ionic charge, $[\mathbf{j}]$ in units of coulombs per square metre per second). On the other hand the second expression, which is more customary, ensures the continuity of the tangential component of \mathbf{j} . In particular, the influence on the conservation of the total charge in the system during the transient process is analysed.

2 Equations

The device consists of a set of thin wires parallel to a grounded iron plate. The wires are brought to a negative potential of high amplitude. The resulting electric field is particularly strong around the wires and causes the acceleration of free electrons which move away from the cathode and combine with atoms. The negative ions drift toward the anode, i.e. the grounded plate, because of Coulomb forces. The model is limited to a box extending from the middle of a wire to half the distance between two consecutive wires (Fig. 1). In the absence of coating particles, the ion drift is described by the equations:

$$\nabla \cdot \mathbf{d} = \rho_i \quad (2)$$

$$\nabla \times \mathbf{e} = 0 \quad (3)$$

$$\mathbf{d} = \varepsilon_0 \mathbf{e} \quad (4)$$

$$\partial_t \rho_i + \nabla \cdot (\mu_i \rho_i \mathbf{e}) = 0 \quad (5)$$

where μ_i is the ion mobility in units of volts per second [2].

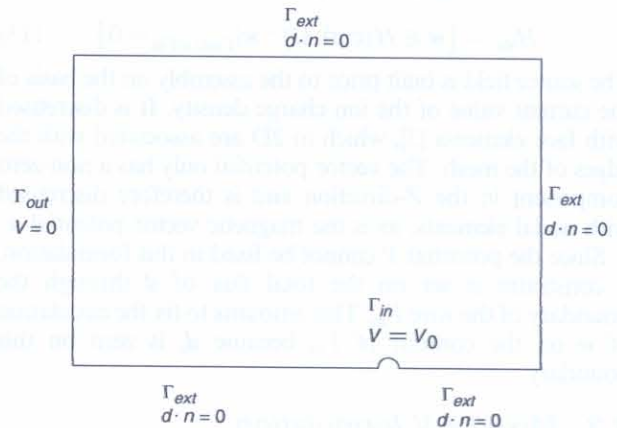


Fig. 1 Boundary conditions for the finite element model of the electrostatic painting device

Equations (2)–(5) define an electrostatic problem coupled with a transient convection problem. They are solved separately: the transient equation is numerically integrated in time and the static problem is solved at each time step. Nonlinear iterations can be avoided if the time step is small enough to ensure a slow evolution of the solution.

3 Electrostatic formulations

3.1 Electric scalar potential V

The classic scalar potential formulation reads as:

find $V \in H_V(\Omega)$ such that:

$$\int_{\Omega} \nabla V' \cdot \nabla V d\Omega - \int_{\Omega} V' \varepsilon_0^{-1} \rho_i d\Omega = 0 \quad (6)$$

$$\forall V' \in H_{V_0}(\Omega)$$

with the function spaces

$$H_V = \{V \in H(\text{grad}, \Omega) : V|_{\Gamma_{in}} = V_0, V|_{\Gamma_{out}} = V_1\} \quad (7)$$

$$H_{V_0} = \{V \in H(\text{grad}, \Omega) : V|_{\Gamma_{in}} = V|_{\Gamma_{out}} = 0\} \quad (8)$$

3.2 Electric vector potential \mathbf{w}

The electric flux density is defined as:

$$\mathbf{d} = \mathbf{d}_s + \nabla \times \mathbf{w} \quad (9)$$

where \mathbf{d}_s is a source field such that $\nabla \times \mathbf{d}_s = \rho_i$ so that (2) is satisfied exactly. The weak formulation reads as:

find $\mathbf{d}_s \in H_{d_s}(\Omega)$ and $\mathbf{w} \in H_w(\Omega)$ such that:

$$\int_{\Omega} \varepsilon_0^{-1} \nabla \times \mathbf{w}' \cdot (\mathbf{d}_s + \nabla \times \mathbf{w}) d\Omega = 0 \quad (10)$$

$$\forall \mathbf{w}' \in H_{w_0}(\Omega)$$

with the function spaces

$$H_{d_s} = \{ \mathbf{d}_s \in H(\text{div}, \Omega) : \mathbf{d}_s|_{\Gamma_{\text{in}} \cup \Gamma_{\text{ext}}} = 0, \nabla \cdot \mathbf{d}_s = \rho_i \text{ in } \Omega \} \quad (11)$$

$$H_w = \left\{ \mathbf{w} \in H(\text{curl}, \Omega) : \nabla \times \mathbf{w}|_{\Gamma_{\text{ext}}} = 0, \int_{\partial \Gamma_{\text{in}}} \mathbf{w} = \varphi_d \right\} \quad (12)$$

$$H_{w_0} = \{ \mathbf{w} \in H(\text{curl}, \Omega) : \mathbf{w}|_{\Gamma_{\text{ext}} \cup \partial \Gamma_{\text{in}}} = 0 \} \quad (13)$$

The source field is built prior to the assembly on the basis of the current value of the ion charge density. It is discretised with face elements [3], which in 2D are associated with the edges of the mesh. The vector potential only has a non-zero component in the Z-direction and is therefore discretised with nodal elements, as is the magnetic vector potential \mathbf{a} .

Since the potential V cannot be fixed in this formulation, a constraint is set on the total flux of \mathbf{d} through the boundary of the wire Γ_{in} . This amounts to fix the circulation of \mathbf{w} on the contour of Γ_{in} because \mathbf{d}_s is zero on this boundary.

3.3 Mixed \mathbf{d} - V formulation

The unknown fields are the scalar potential V and the electric flux density \mathbf{d} . A weak formulation of (2) and (4) is solved:

find $\mathbf{d} \in H_d(\Omega)$ and $V \in H_V(\Omega)$ such that:

$$\int_{\Omega} \nabla V' \cdot \mathbf{d} d\Omega + \int_{\Omega} V' \rho_i d\Omega - \int_{\Gamma_{\text{in}} \cup \Gamma_{\text{out}}} V' \mathbf{d} \cdot \mathbf{n} d\Gamma = 0 \quad (14)$$

$$\forall V' \in H_{V_0}(\Omega), \text{ and}$$

$$\int_{\Omega} \varepsilon_0^{-1} \mathbf{d}' \cdot \mathbf{d} d\Omega + \int_{\Omega} \mathbf{d}' \cdot \nabla V d\Omega = 0 \quad (15)$$

$$\forall \mathbf{w}' \in H_{w_0}(\Omega)$$

with the function space

$$H_d = \{ \mathbf{d} \in H(\text{div}, \Omega) : \mathbf{d}|_{\Gamma_{\text{ext}}} = 0 \} \quad (16)$$

in addition to (7) and (8). Fields V and \mathbf{d} are discretised with nodal and face elements, respectively. The resulting algebraic system takes the form of:

$$\begin{bmatrix} \mathbf{A} & \mathbf{B} \\ \mathbf{B}^T & \mathbf{0} \end{bmatrix} \begin{bmatrix} x_d \\ x_V \end{bmatrix} = \begin{bmatrix} 0 \\ b \end{bmatrix} \quad (17)$$

where x_d and x_V are the unknown degrees of freedom of the fields \mathbf{d} and V . The empty block on the diagonal of the system (17) is characteristic of mixed formulations.

Babuška and Brezzi have proved that the discrete function spaces for the unknown fields of a mixed problem solved with finite elements must satisfy the so-called Babuška-Brezzi (BB) condition [4]. In fluid mechanics, this condition prevents some combinations of shape functions from being used for the velocity and pressure in incompressible Navier-Stokes equations: equal order elements, for example, lead to spurious pressure oscillations.

One possibility is to discretise the pressure and the velocity with first-order and second-order elements, respectively. In order to apply this result to our electrostatic formulation, we should discretise \mathbf{d} with second-order face elements and V with first order nodal elements.

An alternative has been proposed in [5] and [6] where use is made of modified weighting functions in order to circumvent the BB condition. The pressure-stabilised Petrov-Galerkin (PSPG) method allows the velocity and pressure to be discretised with equal order elements. In fluid mechanics, the weighting functions for the momentum equations become:

$$\mathbf{v}' \rightarrow \mathbf{v}' + \tau_e \nabla p' \quad (18)$$

where \mathbf{v} is the velocity, p is the pressure and τ_e is an element-dependent constant free parameter, comparable with the free parameter of the streamline upwind Petrov-Galerkin (SUPG) formulation, which is empirically determined. By analogy, the PSPG method can be applied to the mixed electrostatic formulation by modifying the weighting functions of (15):

$$\mathbf{d}' \rightarrow \mathbf{d}' + \tau_e \nabla V' \quad (19)$$

which amounts to adding the following terms to the left-hand side:

$$\tau_e \int_{\Omega} \varepsilon_0^{-1} \nabla V' \cdot \mathbf{d} d\Omega + \tau_e \int_{\Omega} \nabla V' \cdot \nabla V d\Omega \quad (20)$$

The second advantage of the method is that the structure of the system (17) becomes:

$$\begin{bmatrix} \mathbf{A} & \mathbf{B} \\ (1 + \tau_e) \mathbf{B}^T & \mathbf{C} \end{bmatrix} \begin{bmatrix} x_d \\ x_V \end{bmatrix} = \begin{bmatrix} 0 \\ b \end{bmatrix} \quad (21)$$

which is no longer indefinite. The choice of an appropriate value of τ_e is discussed in Section 5.

4 Time integration schemes

A time integration scheme suitable for convection equations must be chosen for (5). Two schemes based on Padé approximants are used, an explicit ($R_{0,3}$) and an implicit one ($R_{2,1}$).

4.1 Explicit $R_{0,3}$

The Taylor-Galerkin scheme derives from the approximant $R_{0,3}$. It is a third-order function that is accurate and requires a less severe condition on the time step than the Lax-Wendroff scheme [7]. In the multi-step version of the scheme, only first-order derivatives are needed:

$$\rho^{n+1/3} = \rho^n + \frac{1}{3} \Delta t \partial_t \rho^n \quad (22)$$

$$\rho^{n+1/2} = \rho^n + \frac{1}{2} \Delta t \partial_t \rho^{n+1/3} \quad (23)$$

$$\rho^{n+1} = \rho^n + \Delta t \partial_t \rho^{n+1/2} \quad (24)$$

4.2 Implicit $R_{2,1}$

This scheme is unconditionally stable for convection equations [8]. The two-step expression avoids second-order derivatives at the cost of an additional intermediate unknown, $\rho^{n+1/2}$:

$$\rho^{n+1/2} + \frac{2}{3} \rho^{n+1} - \frac{1}{6} \Delta t \partial_t \rho^{n+1} = 0 \quad (25)$$

$$\rho^{n+1} + \Delta t \partial_t \rho^{n+1/2} = \rho^n + \frac{1}{3} \Delta t \partial_t \rho^n \quad (26)$$

5 Results

The different formulations are first studied on a simple test case where the time step and the element size can be easily varied. The purpose is to both determine an optimal value for the free parameter in the stabilised mixed formulation and also to study the convergence of the charge conservation error for the electrostatic formulations. The error is defined as the residual of (5):

$$R_\rho^n = \int_\Omega \rho_i^{n+1} - \rho_i^n d\Omega + \Delta t \int_{\partial\Omega} \mathbf{j} \cdot \mathbf{n} d\Omega \quad (27)$$

which quantifies the difference between the charge which has been gained or lost by the system through its boundaries during the time interval Δt , and the effective variation of the total charge. The relative error r_ρ^n is the residual R_ρ^n divided by the total charge at steady-state conditions. It can be integrated in time to characterise the global error for the whole integration process:

$$r_Q = \sum_{n=1}^{n_{\max}} |r_\rho^n| \quad (28)$$

The real model is then solved to confirm the results obtained with the simple configuration.

5.1 Test model

The test model consists of a rectangular domain. The electric potential is fixed to zero and V_{\max} on the left boundary (Γ_{out}) and the right boundary (Γ_{in}) respectively. The initial distribution of ρ_i is exponential in order to induce an intense electric field near the right boundary, as actually occurs around the wire in the real problem. In order to determine an optimal expression of τ_e for the stabilised $d-V$ formulation, the electrostatic equation is solved for several meshes with a decreasing element size h_e . The number of bi-conjugate gradient (BiCG) steps as a function of τ_e is plotted in Fig. 2 for different values of h_e . The optimal value of τ_e lies for each mesh between zero and -1 and does not vary strongly with h_e . Therefore, a constant value $\tau_e = -0.8$ has been chosen for all computations.

The problem is solved with both explicit and implicit schemes for $\Delta t = 5 \times 10^{-6}$ s, and with the implicit scheme for $\Delta t = 20 \times 10^{-6}$ s. The error r_Q is plotted in Fig. 3. The implicit and explicit time schemes give similar results and

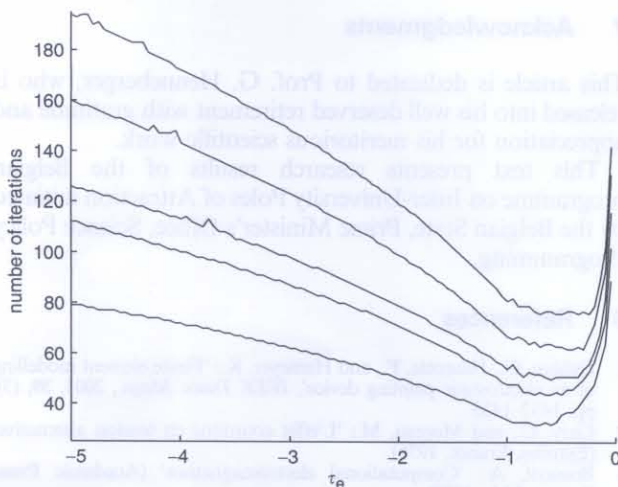


Fig. 2 Test model: number of iterations of the BiCG solver for the stabilised mixed $d-V$ formulation as a function of the parameter τ_e for different values of the element size h_e

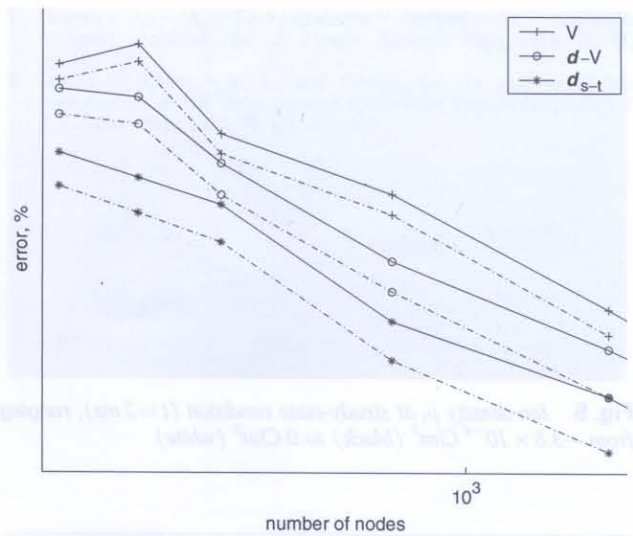


Fig. 3 Test model: relative error r_Q as a function of the number of nodes for the test-case solved with the different electrostatic formulations, with $\Delta t = 5 \times 10^{-6}$ s (continuous lines) and $\Delta t = 20 \times 10^{-6}$ s (dotted lines)

the corresponding curves are identical. It appears that the error is higher when \mathbf{j} is expressed as $\mathbf{j} = \mu\epsilon\rho_i$ (scalar potential formulation) than when expressed as $\mathbf{j} = \mu\epsilon^{-1}\mathbf{d}\rho_i$ (vector potential and mixed formulations). The lowest error is obtained with the vector potential formulation with source field.

5.2 Real model

A uniform charge density $\rho_i = -10^{-9}$ C/m³ is assumed at $t=0$. First, ions are created around the wire and start moving away from it in all directions. At some distance from the wire, the charges are attracted by the plate where they are neutralised. The ionisation phenomenon reaches a steady-state condition after 1 ms (Fig. 4) and after 1.5 ms, the flux of ions reaching the plate compensates the flux of ions leaving the wire to within 1%. From that moment on, the total charge of the system must be constant. The charge density at steady-state and the corresponding source field are represented in Figs. 5 and 6, respectively.

The implicit time integration scheme is used with $\Delta t = 10^{-5}$ s. The explicit scheme is not used because its stability condition $C^2 < 1$, where C is the Courant Friedrichs

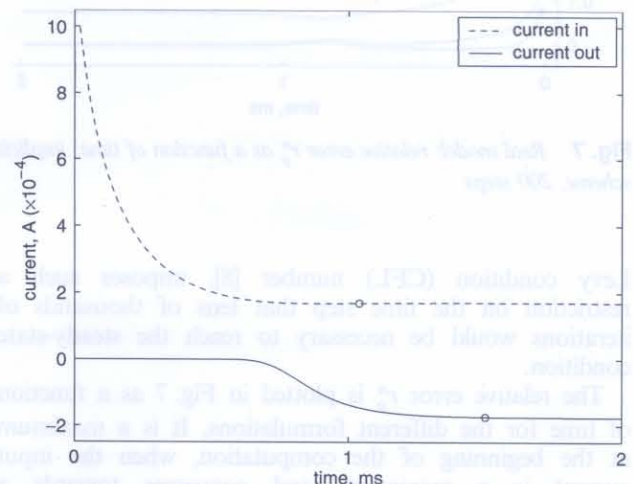


Fig. 4 Real model: ion current flowing through the wire ('in') and the plate ('out'); the 'o' marks the point where the current has reached 99% of its steady-state value

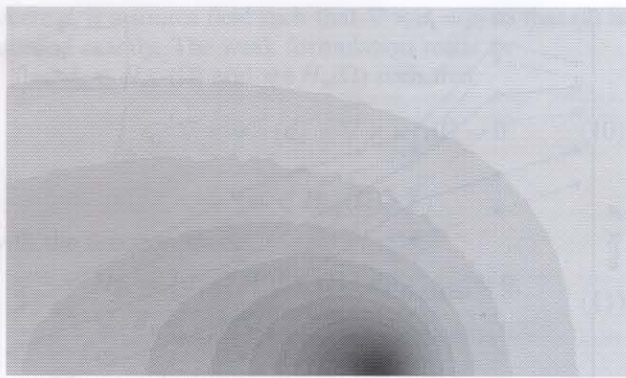


Fig. 5 Ion density ρ_i at steady-state condition ($t=2$ ms), ranging from -3.8×10^{-4} C/m³ (black) to 0 C/m³ (white)

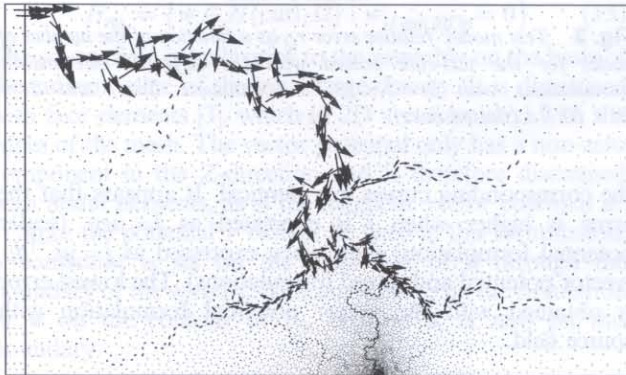


Fig. 6 Source field d_s at steady-state conditions

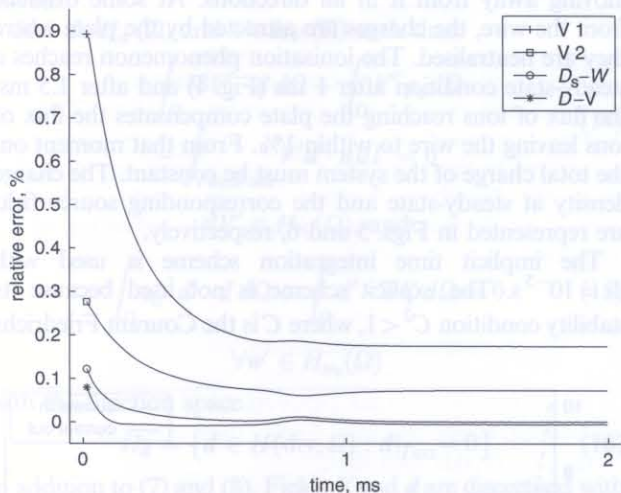


Fig. 7 Real model: relative error r_p^n as a function of time; implicit scheme, 200 steps

Levy condition (CFL) number [8], imposes such a restriction on the time step that tens of thousands of iterations would be necessary to reach the steady-state condition.

The relative error r_p^n is plotted in Fig. 7 as a function of time for the different formulations. It is a maximum at the beginning of the computation, when the input current is a maximum, and converges towards a constant. The largest error occurs for the scalar potential formulation with first-order elements. It decreases when second-order elements are used but remains significantly

Table 1: Comparison of the relative errors r_Q

Formulation	r_Q [%]	Number of degrees of freedom
V , first-order	47.7	n_{node}
V , second-order	17.7	$n_{\text{node}} + n_{\text{edge}}$
$d_s - w$	1.8	n_{node}
$d - V$	1.4	$n_{\text{node}} + n_{\text{edge}}$

higher than the error obtained with the $d - V$ and $d_s - w$ formulations.

The total error r_Q is given in Table 1 with the number of degrees of freedom of each formulation. The formulation with source field ($d_s - w$) is apparently the most interesting, since it is the most accurate and requires only n_{node} unknowns. However, the flux of d that is fixed by the boundary conditions is for this problem an unknown quantity which has to be determined in some way. In this case, the problem is first solved with a scalar potential formulation and φ_d is calculated as the integral of $-\epsilon_0 \nabla V$ on the boundary. On the other hand, the mixed formulation requires more unknowns but the boundary conditions on the potential are easily taken into account, and it is more accurate than the scalar potential formulation with second-order elements.

6 Conclusions

The equations describing the drift of ions in an electrostatic painting device have been presented. Two unusual electrostatic formulations have been proposed in addition to the classic scalar potential formulation: the vector potential formulation with source field ($d_s - w$) and the mixed formulation ($d - V$). A stabilisation technique for mixed problems, originally developed for Stokes problems and known as the PSPG formulation, has been successfully applied to the mixed electrostatic formulation. It has been shown that the formulations ensuring the continuity of the normal component of j , i.e. the vector potential and mixed formulations, lead to a better charge conservation than the scalar potential formulation, even if V is discretised with second-order elements. The mixed formulation has on the vector potential formulation the advantage that the boundary conditions on V can be easily imposed.

7 Acknowledgments

This article is dedicated to Prof. G. Henneberger, who is released into his well deserved retirement with gratitude and appreciation for his meritorious scientific work.

This text presents research results of the Belgian programme on Inter-University Poles of Attraction initiated by the Belgian State, Prime Minister's Office, Science Policy Programming.

8 References

- 1 Deliége, G., Henrotte, F., and Hameyer, K.: 'Finite element modelling of an electrostatic painting device', *IEEE Trans. Magn.*, 2003, **39**, (3), pp. 1432-1435
- 2 Gary, C., and Moreau, M.: 'L'effet couronne en tension alternative' (Eyrolles, France, 1976)
- 3 Bossavit, A.: 'Computational electromagnetism' (Academic Press, Boston, MA, 1998)
- 4 Babuška, I.: 'The finite element method with Lagrangian multipliers', *Numer. Math.*, 1973, **20**, pp. 179-192
- 5 Franca, L.P., and Hughes, T.J.R.: 'A new finite element formulation for computational fluid dynamics: VII. The Stokes problem with

- various well-posed boundary conditions: symmetric formulations that converge for all velocity/pressure spaces', *Comput. Methods Appl. Mech. Eng.*, 1987, **65**, (1), pp. 85–96
- 6 De Mulder, T.: 'Stabilized finite element methods for turbulent incompressible single-phase and dispersed two-phase flows'. PhD Thesis, Katholieke Universiteit Leuven, May 1997
 - 7 Donea, J.: 'A Taylor-Galerkin method for convective transport problems', *Int. J. Numer. Methods Eng.*, 1984, **20**, (1), pp. 101–119
 - 8 Donea, J., Quartapelle, L., and Selmin, V.: 'An analysis of time discretisation in the finite element solution of hyperbolic problems', *J. Comput. Phys.*, 1987, **70**, pp. 463–499